FR8500493

5. International symposium on microstructural characterization of materials
Risoe (Denmark) 3-7 Sep 1984
CEA-CONF--7434

MICROSTRUCTURAL INFORMATION FROM CHANNELING MEASUREMENTS

Y. QUÉRÉ

Centre d'études nucléaires
92260 Fontenay-aux-Roses, France

ABSTRACT

Channeling is sensitive to nearly all structural changes in solids. One briefly recalls how particles are dechanneled by lattice defects and describes the main applications of channeling to materials science : detection of radiation damage, location of impurity atoms, precipitation in alloys...

Channeling being a phenomenon characteristic of perfect crystals, any type of lattice imperfection (phonons, crystal defects, precipitation etc.) is expected to produce dechanneling. Consequently channeling and its opposite, dechanneling, have both been used to study structure and structural changes of materials.

1. GENERALITIES

Positive particles, like protons, α, ions ...., travelling between atomic planes {hkl} or rows <hkl> in a crystal are maintained on stable trajectories thanks to the repulsive potential of the crystal ions (fig. 1). Most of what we know about this phenomenon is described in the classical theory of Lindhard (1965). To summarize in one sentence, we just say here that a channeled particle (later on : c.p.) is maintained in potential valleys (planar channeling) or tubes (axial channeling) provided that its oscillatory (nearly) straight trajectory lies within a small angle (Ψ_c) from the plane (or axis). This c.p. gets dechanneled when its comes too close (within $\simeq a_{TF}$, Thomas Fermi radius) to atomic planes or rows.

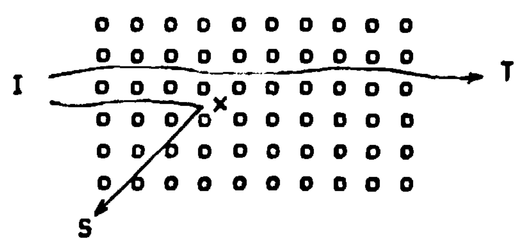

Fig. 1. A channeled incident beam I is altered by the presence of "defect" x (phonon, lattice defect, precipitate..) Part of it (T) is transmitted, part of it (S) is dechanneled and scattered.

This paper is dedicated to Professor Jacov Alpert.

Most of the experiments on channeling have been performed with accelerators, which deliver a beam of (nearly) parallel particles on a target sample, the crystallographic planes (or rows) of which can be aligned along the beam with help of a goniometer. According to the thickness d of the samples, the beam may go through (transmission experiments, Nelson and Thompson, 1963) or be scattered at large angles (back scattering experiments, Picraux et al., 1969). The proportion of transmitted (or back scattered) particles depends drastically on the quality of the channeling conditions.

One may also use randomly distributed particles from a radioactive source and choose d such that only the channeled particles are transmitted : here the crystal it self plays the role of the goniometer (channelographic method, Quéré, 1970).

2. STUDY OF LATTICE DEFECTS

To be able to interpret correctly a dechanneling experiment, it is generally necessary - or at least useful - to know the behaviour of a channeled beam facing a specific type of defect. We shall first describe briefly the influence of some of the most frequent defects.

2.1. Free surfaces. A free surface in a crystal tends to dechannel c.p.'s because of the presence of Rutherford scattering centers (nuclei) at the surface.

Microscopic cavities (radius R) in solids provide a good example of this kind of dechanneling. A c.p. arriving on a cavity leaves for a while the crystal and re-enters after a straight trajectory of length ℓ ($0 < \ell < 2R$). This reentrance, although attempted at an angle smaller, by construction, than Ψ_c, is successful only if it takes place far enough of a nucleus. This case can be analyzed simply (Ronikier, 1975) and gives rise to an energy-(E) independant dechanneling probability or cross section (see also § 3.7).

2.2. Grain- or twin- boundaries. In this case, the dechanneling is practically total : the dechanneling cross section is equal to the area $\mathcal{A}$ of the boundary. This dechanneling has been observed in many cases (Quéré, Resneau and Mory, 1966). Examples may be found on fig. 2 and also further on fig.10.

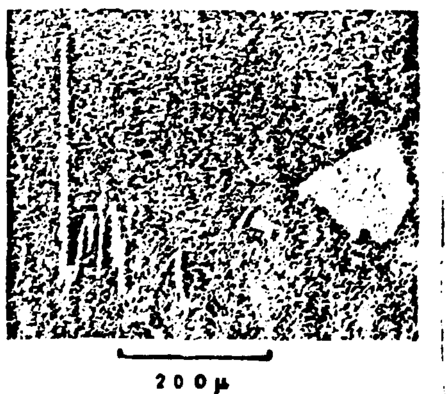

Fig. 2. Grain - and twin - boundaries seen in platinum by transmission channelograph. The particles are fission fragments (≈ 60-100 MeV) of uranium. Dechanneling by boundaries (white contrast) is clearly visible (Mory and Delsarte, 1968).

2.3. Stacking faults. This defect consists of a shift of one part of the crystal with respect to the other. It is simple enough to allow precise theoretical description. The dechanneling cross sections are found to be E-independant and to have values of the order of $0.2\,\mathcal{A}$ (case of α particles in gold, Mory, 1976) in very close agreement with experimental determination (Mory and Quéré, 1972). Observations of this type of dechanneling has been frequently reported (Schober and Balluffi, 1968 ...).

2.4 Antiphase boundaries. In an ordered alloy, planes (or rows) of type α, β, α... may be shifted to β, α, β... at an "antiphase boundary". The chemical composition of α and β being generally different, the (unsymmetrical) potential valleys α-β, shifted to β-α, give rise to dechanneling on the boundary (see fig. 3). This dechanneling has been observed in the case of ordered Cu_3Au alloys (Chevallier, 1974), cross sections being about 0.3 Å for α particles.

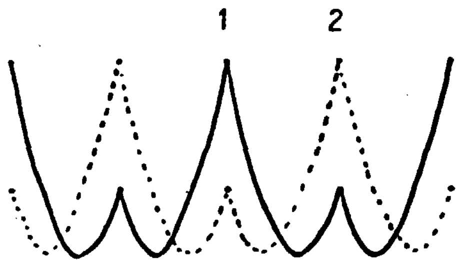

Fig. 3. Potential valleys of planar channeling in an ordered alloy with neighnouring planes of different chemical composition (1). Beyond an antiphase boundary, the valleys are shifted to (2), giving rise to dechanneling.

2.5 Dislocations. In the previous cases, dechanneling was due to an abrupt change (shift and/or rotation) of the channeling valleys forcing some of the c.p.'s to "hit" the cores (of radius ≃ a_{TF}) of the atoms of the crystal. The case of dislocations is slightly different : the alteration of the crystal by a dislocation is not abrupt but continuous, the curvatures due to the defect covering long distances. Anyhow, as a first guess, one may treat a dislocation as a tube inside (resp. outside) of which dechanneling is complete (resp. negligible), dechanneling being due to the centrifugal forces exerted on the c.p. by the curvature of the crystal.

Such analytical treatments (Quéré, 1968) applied to straight dislocations give dechanneling widths with a $E^{1/2}$ energy dependance and of the order of 100 A for α particles, with essentially no specific loss of energy for the non-dechanneled particles (Pathak, 1975) (see fig. 4). Computer simulations generally confirm this $E^{1/2}$ dependance but with numerical values, for the width, typically half of the previous ones (Kudo, 1980). If the dislocation is not straight but curved (like in the frequent case of dislocation loops) a strong decrease of the dechanneling cross section is expected (Quéré, 1978) and observed (Merkle et al., 1973, Chalant and Mory, 1979).

Dechanneling by dislocations has been observed (see fig. 4) and measured by many authors either by transmission (Leteurtre et al. 1971) or by back scattering (Picraux et al. 1978 ; Mannami et al. 1980). Especially the energy

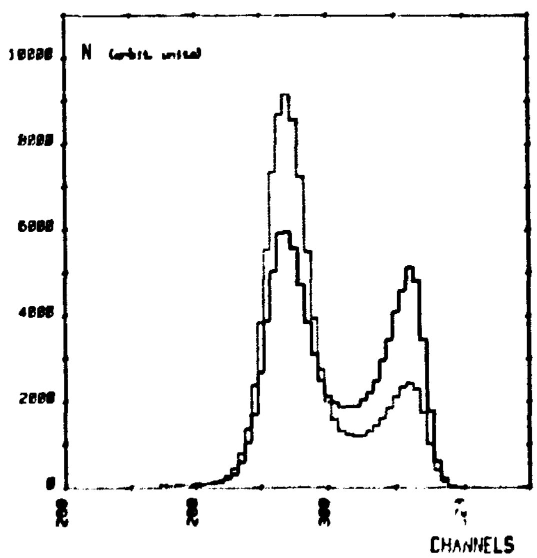

Fig. 4. Transmission spectra of 3.6 MeV protons through (110) planes of a 6 μm thick crystal of tantalum before (——) and after (...) cold working. On the right, the channeled peak is altered in intensity, not in energy (Bhattacharya et al. 1980).

dependance has been measured carefully, having frequently the $E^{1/2}$ dependance predicted by Quéré (1968) (see fig. 5). Anyhow, this dependance goes down more or less to $\simeq E^{1/4}$ when dislocations are strongly dissociated, in which case part of the dechanneling is of dislocation type ($E^{1/2}$) and part of stacking fault type (E^{0} : see § 2.3.). It was even suggested by Kimura et al. (1980) that the exponent of E could give an indication on the separation of partial dislocations i.e. on the stacking fault energy.

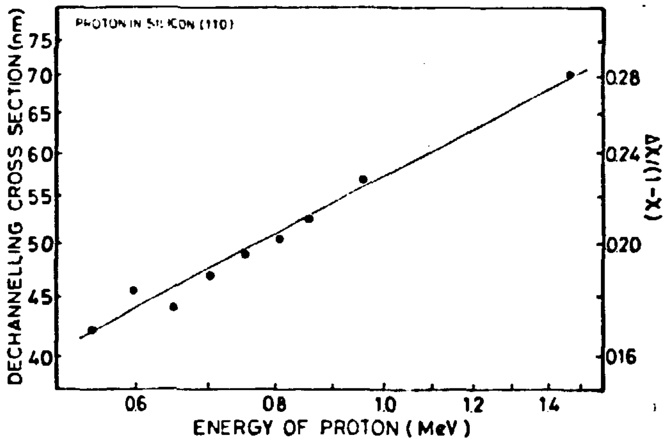

Fig. 5. Dependence of the dechanneling and the dechanneling cross section of dislocations on the energy of the channeled particles in (110) planes of silicon (Mannami et al. 1980).

2.6. Point defects. Vacancies are not expected to give rise to any observable dechanneling, whereas interstitials are in right position to dechannel quite efficiently. The dechanneling due to an atom lying in the center of a channel might vary with energy like $E^{-1/2}$ (Quéré, 1974). Typical dechanneling cross sections of a hydrogen interstitial impurity for α particles in Pd are $\simeq 6 \times 10^{-3}$ Å^2 in good agreement with calculated values (Quillico, Jousset, 1975 ; see also fig. 6).

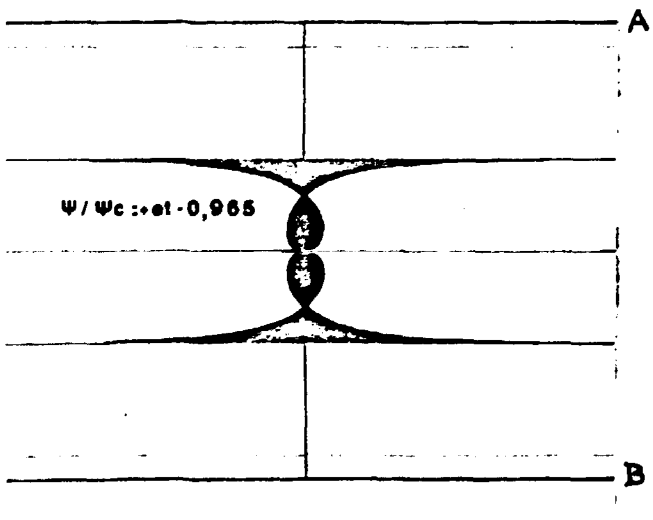

Fig. 6. Dechanneling regions (in black) around a punctual scattering center situated in the middle between two planes (A and B) for a typical value of the ratio Ψ/Ψ_c (Ψ : maximum oscillation angle ; Ψ_c : critical angle). (Mory, 1976).

3. CHANNELING : A TOOL TO STUDY MATERIALS

3.1. Determination of crystal orientation. The back scattering of dechanneled c.p.'s is accompanied by an effect of shadow called "blocking" which has been used to build a crystal orientation blocking chamber using protons (Tulinov, 1966).

A still more direct method consists of using ponctual radioactive sources. The particles entering a crystal will be preferentially transmitted by channeling between the atomic planes of low indices. After transmission, these c.p.'s create, on a plate, a channeling pattern which gives the traces of the real planes of the structure : for example the image of gallium shown on fig. 7 is the image of the direct - not the reciprocal - lattice (see also Delsarte, 1970).

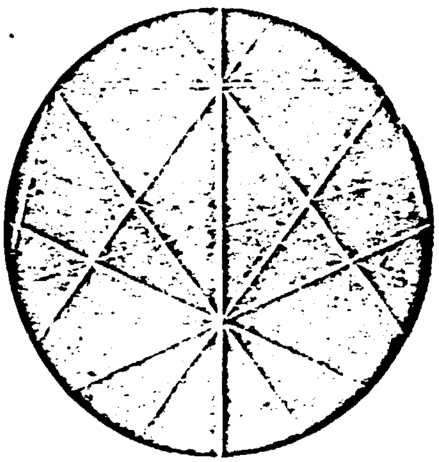

Fig. 7. Channeling pattern of α particles transmitted through a gallium single crystal, at T = 4.2 K. Indices of planes will be found in Takahashi and Mory (1981).

3.2. Observation of radiation damage in crystals. Ion implantation has become an increasingly important method to dope semiconductors or to modify the surface properties of alloys. Anyhow the defects created by the slowing down of implanted species may alter severely the properties of the host crystal. Channeling offers a simple means to detect - generally in the implanter system itself - both the location of implanted ions (see § 3.3.) and the presence of radiation damage as shown on fig. 8.

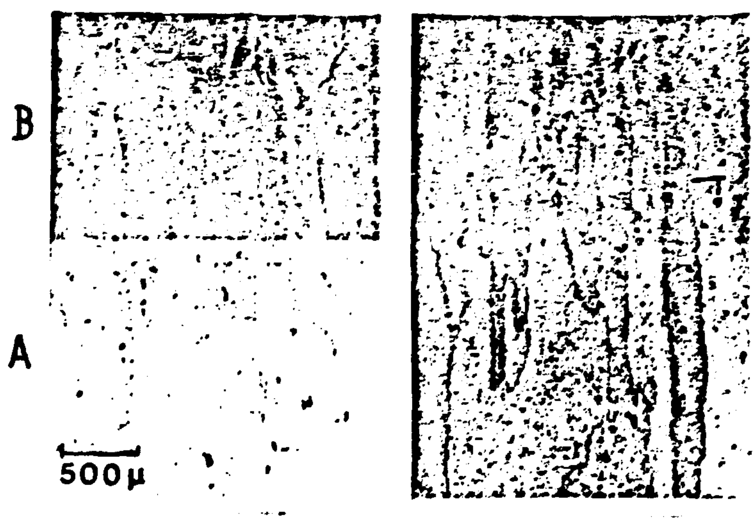

Fig. 8. A low magnification overall view of dechanneling by irradiation defects. A tantalum polycrystal has been irradiated by 3 MeV protons (region A). Transmission channelographs of protons show a dramatic variation of dechanneling between region A and the non irradiated region B. This dechanneling is due to dislocation loops in A. Elongated grains are visible both in A and in B.

Left : high dose of irradiation,
Right : low dose.

Although quantitative studies in this field are subject to criticism and should not be too ambitious (Quéré, 1976), such experiments by back scattering allow semi-qualitatively a description of the damage profiles and also the observation of the thermal annealing stages (Bøgh, 1969) ; Nashiyama, Pronko and Merkle, 1976 ; Grob and Siffert, 1983 ...). They also allow to observe the production of damage as a function of irradiation dose. But one should not forget that the "shadow" of defects on each other induce a rapid saturation of dechanneling (i.e. a rapid opacity of irradiated samples to c.p.'s) long before defect saturation is built up (Jousset and Lorenzelli, 1973, see fig. 9).

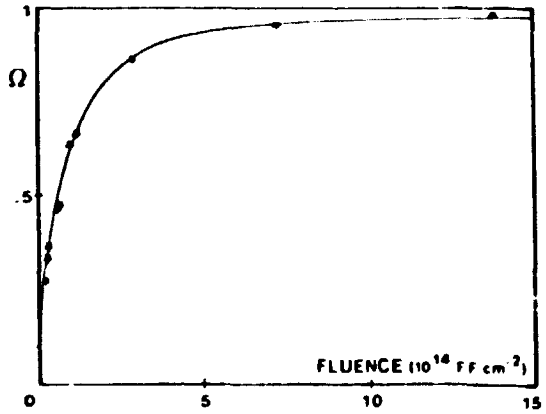

Fig. 9. Variation of dechanneling $\dot{\Omega}$ of α particles versus irradiation fluence in iron samples irradiated with fission fragments at 20 K (Jousset and Lorenzelli, 1973).

3.3. Lattice location of atoms. If the cross x of fig. 1 is taken to be an atom (or an ion), it is clear that channeling is affected by x along <10> whereas it is not along <11>. More generally, a study of dechanneling conditions along various directions of a crystal A containing atoms B allows in principle to "locate" the B atoms in the A lattice (Bøgh, 1967).

This technique has been used extensively, particularly to locate dopants in semiconductors (see for instance Feldman, 1973), hydrogen in metals (Picraux, 1975) etc. For example, in f.c.c. metals, hydrogen has been found to sit on octahedral sites with, in some cases (Pd, Pt, Al), a possible transition octahedral → tetrahedral when temperature increases (Bugeat, 1979). In semiconductors, a number of transitions substitutional → interstitial have been reported (Davies, 1970 ; Wiggers and Saris, 1977 ...).

The case of compound semiconductors like Ga As, where impurity atoms like Si are generally found substitutional, raises an interesting question : are these atoms on the Ga or on the As sublattice ? Here, the asymetry of potential valleys like <110> observed by Bontemps, Fontenille and Guivarc'h (1976) makes it possible to answer this question. For example, S or Sb occupy the As sublattice ; In occupies the Ga sublattice ; whereas Si lies in equal concentrations on both sublattices (Bhattacharya and Pronko, 1983 ; Andersen, Chechenin, Timoshnikov and Zhang, 1984).

3.4. Configuration of trapped interstitials. The self-interstitial, produced by irradiation, has a split <100> configuration in f.c.c. metals. If solute impurities are present in, say, copper, interstitials may become trapped on these impurities either without displacing them from their sites (case i/) or by forming a mixed Cu-impurity split entity (case ii/).

This alternative has been studied in Al containing Mn, Zn, Ag or Sn (Swanson and Maury, 1975) and in Cu containing Ag, Sb or Au (Swanson et al., 1976). In both cases backscattering of c.p.'s on the heavy impurity is studied versus the temperature of annealing of the irradiated alloy. Some configurations (like Al-Mn, Al-Zn or Al-Ag) exhibit the mixed dumbbell configuration (case ii/) whereas some interstitials (like Cu-Cu in Cu-Ag or Cu-Au) keep their identity while being trapped (case i/).

3.5 Surface relaxation effects. Atoms on the surface of a solid displaced from their normal lattice site, provide a "shadow" in the channels of low-index directions. A backscattering experiment for particles arriving along these directions exhibits a yield peak from which these displacements can be determined. For example, Davies et al. (1976) have observed outward relaxations of ≈ 0.3 Å of platinum atoms on a platinum surface covered by a monolayer of oxygen.

3.6 Recrystallization and self diffusion. During the process of recrystallization, the orientation of grains changes and the concentration of dislocations decreases, two reasons which alter drastically the channeling conditions (fig. 10). This remark has been used to study by transmission of α particles, the kinetics of recrystallization of platinum (Quéré and Couve, 1968) and to determine the Avrami exponent and the recrystallization energy (2.85 ± 0.15 eV) close to the self diffusion energy (2.89 eV).

Fig. 10. Channelograph of a polycrystal of nickel cold worked along xx' and then annealed at 1000°C. Both dechanneling (of protons) by dislocations,and beginning of recrystallization, are clearly visible (Quéré and Uggerhøj, 1976).

By measuring the isothermal evaporation kinetics of dislocation loops in quenched and annealed aluminium, Chalant and Mory (1979) could measure the self diffusion energy in this metal (1.32 ± 0.10 eV).

3.7 Coalescence of gas bubbles. Gas bubbles are formed in solids implanted with rare gases like He. At equilibrium, and for isotropic solids, the bubbles are spherical (radius : R) and the gas pressure is $p \approx 2\gamma/R$ (γ : surface tension). If we write equation $pV = n\,kT$ (V : volume of the bubble $\approx R^3$; n = number of gas atoms in the bubble), it is clear that the surface (not the volume) of the bubble is proportionnal to n. If now, for a fixed total number of implanted gas atoms, we allow the bubbles to coalesce, the total free surface in the solid is thus expected to remain a constant.

Channeling makes it possible to measure, in a very global way, the internal free surface (see § 2.1.). Fig. 11 shows the variation of transmission de-

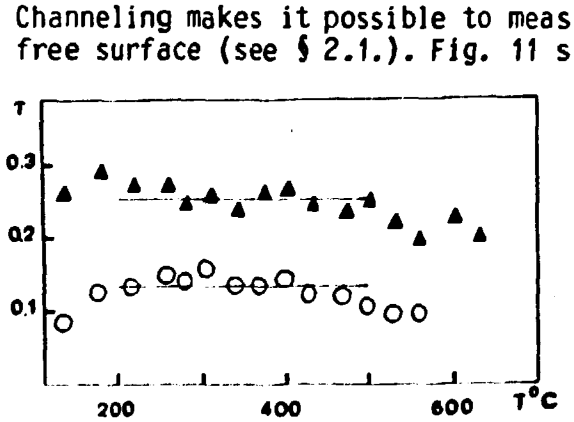

Fig. 11. Transmission τ ($\tau = 1 - \Omega$; Ω : dechanneling) of α channeled particles in helium implanted aluminium versus annealing temperature for two different implantation doses (Ronikier et al., 1975).

channeling (α particles) in a Al sample containing two different quantities of helium condensed into bubbles, as a function of temperature (Ronikier et al., 1975). When T increases, the bubbles tend to coalesce, their number being decreased by a factor of ≃ 10 between 20 and 600°C. In spite of this considerable alteration of bubble density, the dechanneling remains approximately constant, a result in favour of the above mentioned law of constant surfaces.

Let us mention that in this experiment, the probability of dechanneling at a free surface (for planar channeling) is equal to (0.27 ± 0.09) as compared to calculated value of 0.24.

3.8. Precipitation phenomena. Precipitation of a second phase β from a solid solution A-B gives most generally rise to dechanneling, due to boundary creation and/or lattice distortion. The measurement of this dechanneling may help to determine the solubility limits of B and the formation kinetics of β.

For example Whitton et al. (1976) have studied the precipitation of hydride in Nb-H (and Nb-D) by backscattering of He ions. The backscattering yield increases abruptly as soon as precipitation occurs when the temperature is lowered (see fig. 12). The sensitivity of c.p.'s to the lattice distortions in the vicinity of coherent β-phase precipitates gives better determination of the solubility-temperature curves than other methods. The heat of solution of H in Nb was found equal to 0.12 eV/atom, without observable difference between H and D.

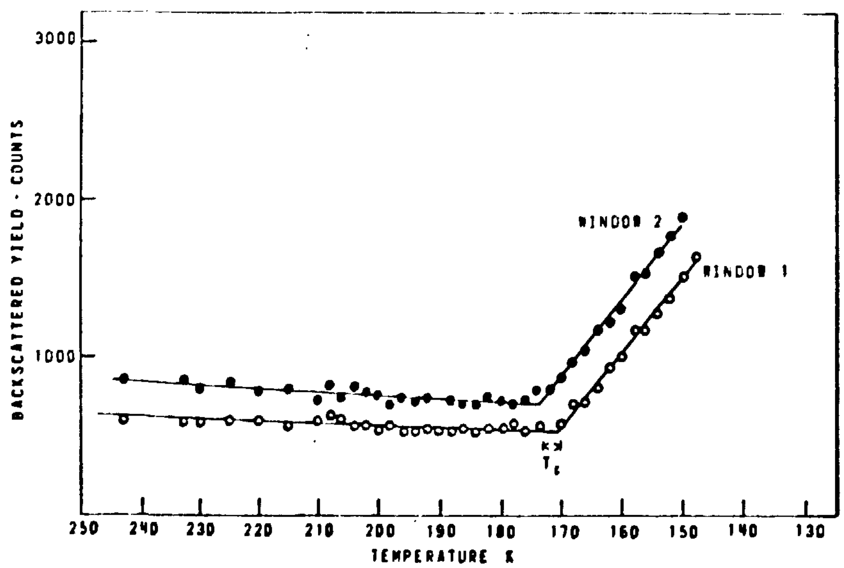

Fig. 12. Effect of cooling on the backscattered yield of 1 MeV channeled He ions in niobium containing 0.33 at % of hydrogen (Whitton et al., 1976).

Another example is the study of Guinier-Preston (G.P.) zones in Al-Cu alloys (Désarmot and Quéré, 1980). The formation of these zones during room temperature ageing of quenched alloys (quenching temperature : θ_T) gives rise to a strong dechanneling. Fig. 13 shows this dechanneling (measured in transmission by the channelographic method) for various values of θ_T. Simple arguments about the dechanneling processes at G.P. zones and analysis of the kinetics give arguments in favour of a spinodal decomposition of the solid solution.

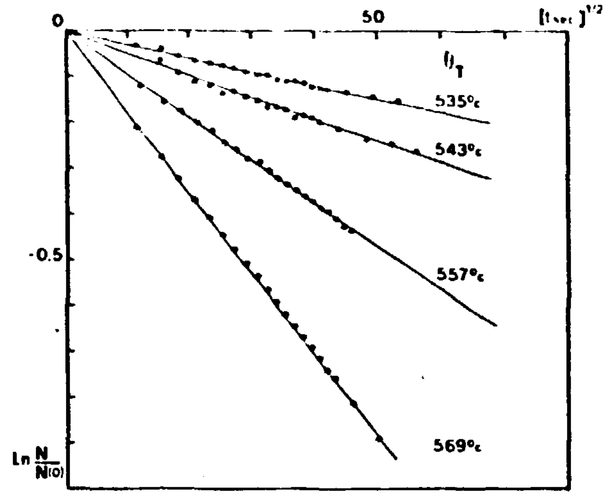

Fig. 13. Logarithm of transmission of channeled α particles versus (ageing time at room temperature)$^{1/2}$ for an Al-4% Cu alloy quenched from various temperatures (Désarmot and Quéré, 1980).

<u>3.9. Characterization of polycrystalline layers.</u> Evaporated Pd on <111> Si substrates transforms into a polycrystalline layer of Pd_2Si upon heat treatment. Channeling measurements on such Pd_2Si layers allowed Sigurd et al. (1973) to observe and to measure the spread in orientation of the crystallites. This spread was found to decrease strongly when the heat treatment temperature was increased.

REFERENCES

Andersen, J.U., Chechenin, N.G., Timoshnikov, Yu.A. and Zhang, Z.H. (1984). Rad. Eff., in press.

Bhattacharya, P.K., Chevallier, J., Uggerhøj, E., Mory, J. and Quéré, Y. (1980). Rad. Eff. 51, 127.

Bhattacharya, R.S. and Pronko, P.P. (1983). Nucl. Inst. Meth. 218, 515.

Bøgh, E. (1967). Interaction of rad. with solids, (Plenum), 361.

Bøgh, E. (1969). Proc. Roy. Soc. A 311, 35.

Bontemps, A., Fontenille, J. and Guivarc'h, A. (1976). Phys. Letters, 55 A, 373.

Bugeat, J.P. (1979). Thèse, Univ. de Grenoble.

Bugeat, J.P. and Ligeon, E. (1979). Phys. Lett. 71 A, 193.

Chalant, G. and Mory, J. (1979). J. Physique lettres, 40, 473.

Chevallier, J. (1974). Unpublished results.

Davies, J.A. (1970). In Phys. of ionized gases, ed. Navinsek (herceg-Novi),34.

Davies, J.A., Jackson,D.P., Mitchell, J.B., Norton, P.R. and Tapping, R.L. (1976). Nucl. Inst. Meth. 132, 609.

Delsarte, G. (1970). Rapport CEA-R-4027.

Désarmot, G. and Quéré, Y. (1980). Acta Met. 28, 1375.

Feldman, L. (1973). In Proc. of the 1973 conference on atomic collisions.

Grob, J.J. and Siffert, P. (1983). Nucl. Inst? Meth.

Jousset, J.C. and Lorenzelli, N. (1973). J. Physique Coll. C-5, suppl.11-12 34.

Jousset, J.C., Mory, J. and Quillico, J.J. (1974). J. Physique Lettres, 35, 229.

Kimura, K., Mannami, M., Kyoshima, A. and Matsushita, M. (1980). Jap. J. Appl. Phys. 19, 733.

Kudo, H. (1980). Nucl. Inst. Meth. 170, 129.

Leteurtre, J. Housseau, N. and Quéré, Y. (1971). J. Physique 32, 205.

Lindhard, J. (1965). Math-Fys. Meddr. 34, 1.
Mannami, M. Kimura, K., Kyoshima, A., Matsushita, M. and Natsuaki, N. (1980). J. Phys. Soc. Jap. 49, 2319.
Merkle, K.L., Pronko, P.P., Gemmell, D.S., Mikkelson, R.C. and Wrobel, J.R. (1973). Phys. Rev. 8, 1002.
Mory, J. (1976). Rapport CEA-R-4745.
Mory, J. and Delsarte, G. (1969). Rad. Eff. 1, 1.
Mory, J. and Quéré, Y. (1972). Rad. Eff. 13, 57.
Mory, J. and Ligeon, E. (1982). J. Mat. Sc. 17, 925.
Nashiyama, I., Pronko, P.P. and Merkle, K.L. (1976). Rad. Eff. 29, 95.
Nelson, R.S. and Thompson, M.W. (1963). Phil. Mag. 8, 1677.
Picraux, S.T. (1975). Proc. Int. Conf. on Ion Beam Surface Layer Analysis, Karlsruhe, 1975.
Picraux, S.T., Davies, J.A., Eriksson, L., Johansson, N.G.E. and Mayer, J.M. (1969). Phys. Rev. 180, 873.
Quéré, Y. (1968). Phys. Stat. Sol. 30, 713.
Quéré, Y. (1970). Ann. Physique, 5, 105.
Quéré, Y. (1974). J. Mat. Nucl. 57, 262.
Quéré, Y. (1976). Rad. Eff. 28, 253.
Quéré, Y. (1978). Rad. Eff. 38, 131.
Quéré, Y., Resneau, J.C. and Mory, J. (1965). Comptes Rendus. 262, 1528.
Quéré, Y. and Couve, H. (1968). J. Appl. Phys. 39, 1197.
Quéré, Y. and Uggerhøj, E. (1976). Phil. Mag. 34, 1197.
Quillico. J.J. and Jousset, J.C. (1975). Phys. Rev. 11, 1791.
Ronikier, D., Désarmot, G., Housseau, N. and Quéré, Y. (1975). Rad. Eff. 27, 81.
Sigurd, D., Bower, R.W., Van Der Weg, W.F. and Mayer, J.W. (1973) Thin Sol. Films, 19, 319.
Schober, T. and Balluffi, R.W. (1968). Phys. Stat. Sol. 27, 195.
Swanson, M.L. and Maury, F. (1975). Canad. J. Phys. 53, 1117.
Swanson, M.L., Howe, L.M. and Quenneville, A.F. (1976). Rad. Eff. 28, 205.
Takahashi. J. and Mory, J. (1981). Comptes Rendus. 292, 1123.
Tulinov, A.F. (1966). Soviet Phys. Usp. 8, 864.
Whitton, J.L., Mitchell, J.B., Schober, T. and Wenzl, H. (1976). Acta Met. 24, 490.
Wiggers, L.W. and Saris, F.W. (1977). Proc. Int. Conf. on Ion Beam Analysis, in Nucl. Inst. Meth.